NASA/TM—2019-220353 AIAA–2019–4499

A Control Strategy for Turbine Electrified Energy Management

Jonathan L. Kratz, Dennis E. Culley, and George L. Thomas
Glenn Research Center, Cleveland, Ohio

October 2019

NASA STI Program . . . in Profile

Since its founding, NASA has been dedicated to the advancement of aeronautics and space science. The NASA Scientific and Technical Information (STI) Program plays a key part in helping NASA maintain this important role.

The NASA STI Program operates under the auspices of the Agency Chief Information Officer. It collects, organizes, provides for archiving, and disseminates NASA's STI. The NASA STI Program provides access to the NASA Technical Report Server—Registered (NTRS Reg) and NASA Technical Report Server—Public (NTRS) thus providing one of the largest collections of aeronautical and space science STI in the world. Results are published in both non-NASA channels and by NASA in the NASA STI Report Series, which includes the following report types:

- TECHNICAL PUBLICATION. Reports of completed research or a major significant phase of research that present the results of NASA programs and include extensive data or theoretical analysis. Includes compilations of significant scientific and technical data and information deemed to be of continuing reference value. NASA counter-part of peer-reviewed formal professional papers, but has less stringent limitations on manuscript length and extent of graphic presentations.

- TECHNICAL MEMORANDUM. Scientific and technical findings that are preliminary or of specialized interest, e.g., "quick-release" reports, working papers, and bibliographies that contain minimal annotation. Does not contain extensive analysis.

- CONTRACTOR REPORT. Scientific and technical findings by NASA-sponsored contractors and grantees.

- CONFERENCE PUBLICATION. Collected papers from scientific and technical conferences, symposia, seminars, or other meetings sponsored or co-sponsored by NASA.

- SPECIAL PUBLICATION. Scientific, technical, or historical information from NASA programs, projects, and missions, often concerned with subjects having substantial public interest.

- TECHNICAL TRANSLATION. English-language translations of foreign scientific and technical material pertinent to NASA's mission.

For more information about the NASA STI program, see the following:

- Access the NASA STI program home page at http://www.sti.nasa.gov

- E-mail your question to help@sti.nasa.gov

- Fax your question to the NASA STI Information Desk at 757-864-6500

- Telephone the NASA STI Information Desk at 757-864-9658

- Write to:
  NASA STI Program
  Mail Stop 148
  NASA Langley Research Center
  Hampton, VA 23681-2199

NASA/TM—2019-220353 AIAA–2019–4499

A Control Strategy for Turbine Electrified Energy Management

Jonathan L. Kratz, Dennis E. Culley, and George L. Thomas
Glenn Research Center, Cleveland, Ohio

Prepared for the
Propulsion and Energy Forum and Exposition
sponsored by the American Institute of Aeronautics and Astronautics
Indianapolis, Indiana, August 19–22, 2019

and

Prepared for the
AIAA/IEEE Electric Aircraft Technologies Symposium (EATS)
cosponsored by AIAA and IEEE
Indianapolis, Indiana, August 22–24, 2019

National Aeronautics and
Space Administration

Glenn Research Center
Cleveland, Ohio 44135

October 2019

Acknowledgments

The authors would like to acknowledge the Transformational Tools & Technologies (TTT) project under the NASA Aeronautics Research Mission Directorate (ARMD) that has supported this work. The authors would also like to acknowledge those within NASA who contributed to creation of the AGTF30 model that was utilized in this study including Jeffryes Chapman and Scott Jones.

This work was sponsored by the
Transformative Aeronautics Concepts Program.

Level of Review: This material has been technically reviewed by technical management.

Available from

NASA STI Program
Mail Stop 148
NASA Langley Research Center
Hampton, VA 23681-2199

National Technical Information Service
5285 Port Royal Road
Springfield, VA 22161
703-605-6000

This report is available in electronic form at http://www.sti.nasa.gov/ and http://ntrs.nasa.gov/

A Control Strategy for Turbine Electrified Energy Management

Jonathan L. Kratz, Dennis E. Culley, and George L. Thomas
National Aeronautics and Space Administration
Glenn Research Center
Cleveland, Ohio 44135

Abstract

Hybrid-electric propulsion architectures provide the infrastructure to enable additional benefits to the propulsion system that are otherwise unrealizable with the sole use of the current, state-of-the-art, gas-driven, turbine engines. The presence of electric machines (EMs) coupled to the shaft(s) of the turbine engine provide the ability to actively alter the operation of the engine to the benefit of the propulsion system and the aircraft it propels. This is the goal of the Turbine Electrified Energy Management (TEEM) concept, which at its broadest level addresses the management of energy across the electrified propulsion system. Prior work has demonstrated the use of this concept to alter steady-state operation and improve transient operability of a hybrid-electric propulsion system. The main benefits previously illustrated include the elimination of stability bleeds and expansion of the turbomachinery design space in order to enable more efficient designs. This paper focuses on the development of control strategies to implement the TEEM concept, and it explores several possible architecture variants for applying this concept. Comparison studies are conducted between a purely gas-driven turbofan (baseline engine configuration) and TEEM augmented variants of the baseline engine. The variants are distinguished by the shaft(s) that possess an EM. The configurations consider EMs on both shafts, an EM on the high pressure spool (HPS) only, and an EM on the low pressure spool (LPS) only. These configurations are referred to as the dual-spool configuration, the HPS configuration, and LPS configuration, respectively. The studies expose several options in configuring and controlling the system, including the use of a single EM coupled to a single shaft of a two-spool engine to positively impact the operability of both shafts. The studies also demonstrate the use of independently designed controllers for the electric machine(s) that allow for a decoupled control design process.

Nomenclature

C	control transition factor
dT	difference between the standard atmospheric temperature and current ambient temperature, °R
$\bar{e}$	normalized error
F_C	fraction of the power extracted from the low pressure spool that is applied to the high pressure spool during decelerations in the dual-spool configuration
F_{VHEP}	very high engine power, power modifier for the super-capacitor charging schedule
F_{VHA}	very high altitude power, power modifier for the super-capacitor charging schedule
m	low pressure compressor pressure ratio set-point controller modifier
MN	Mach number
N_{HPS}	speed of the high pressure spool, rpm
N_{LPS}	speed of the low pressure spool, rpm
P_C	charging power, hp
P_{HPS}	shaft power supplied or extracted by the high pressure spool electric machine, hp
P_{LPS}	shaft power supplied or extracted by the low pressure spool electric machine, hp
P_{sched}	power scheduled for charging the super-capacitor (without modifiers), hp
PLA	power lever angle, °
PLA_{max}	maximum power lever angle, °
PLA_{min}	minimum power lever angle, °
p3	total high pressure compressor discharge pressure, psi
ps3	static high pressure compressor discharge pressure, psi
SM	stall margin, %
T4	high pressure turbine inlet temperature, °R
$t_{r,approx}$	approximate thrust response time, s
t_s	controller time-step, s
τ_{HPS}	torque applied to the high pressure spool, ft-lb_f

τ_{LPS}	torque applied to the low pressure spool, ft-lb_f
V_n	normalized super-capacitor voltage
V_{SC}	super-capacitor voltage, V
$V_{SC,max}$	maximum enforced super-capacitor voltage, V
w_f	fuel flow rate, lb_m/s
$w_{f,max}$	maximum fuel flow at the current Mach number and altitude, lb_m/s
$w_{f,min}$	minimum fuel flow at the current Mach number and altitude, lb_m/s
$w_{f,norm}$	normalized fuel flow
$w_{f,sens}$	sensed fuel flow, lb_m/s

I. Introduction

The prospect of using hybrid-electric propulsion to propel aircraft offers the potential for significant improvements in efficiency, performance, and operability. To date, much of the focus in literature has been on the development and evaluation of new hybrid electric propulsion concepts and their vehicles (Refs. 1 to 5). In these efforts, the flexibility inherent with hybrid-electric architectures is utilized to achieve vehicle level benefits. A common theme is the use of electrically driven propulsors located in opportune positions on the aircraft to achieve aerodynamic benefits (Refs. 6 and 7) and higher propulsive efficiency. In these analyses, it becomes apparent that the focus is primarily on the electrical system or the integration of electrically driven propulsors into the airframe. The turbomachinery is assumed to be a given, and the electrical system is viewed as the novel means for producing benefits for the vehicle. This viewpoint fails to consider the impact that the electrical system can have on the turbomachinery and thus leaves potential benefits on the table. Furthermore, it ignores potential transient operability issues that could arise from instantaneous changes in loads placed on the turbomachinery. Thus, the question is posed, how can the electrical system be used to benefit the turbomachinery performance and preserve its operability?

Turbine Electrified Energy Management (TEEM) is a technology that seeks to use an electrified engine architecture to the benefit of the turbomachinery (Ref. 8). At its broadest level, the TEEM concept is about managing energy in the propulsion system. This is done mainly through the use of electric machines (EMs) coupled to the engine shafts and connected to an electrical power distribution system that includes energy storage. The EMs have the ability to deliver power to, or extract power from, the engine shaft(s) to supplement the power provided by the fuel that is combusted in the burner, thus allowing the engine's operation to be altered by the EM(s). TEEM can be viewed as an operability technology. Steady-state operability can be altered by the EM(s) in given scenarios to provide desired benefits. Potential benefits are believed to include, but are not limited to, the following: the reduction or elimination of stability bleeds and complex variable geometries; the ability to emulate variable cycle operation and to be used in conjunction with multiple flow paths to achieve more efficient variable cycle operation; and the expansion of the engine's operating range to enable new modes and concepts of operation. The other benefit to consider is transient operability in which the EMs are used to alter the dynamic response of the engine. Improving transient operability relaxes constraints on the engine design, which otherwise drive design decisions that incorporate an excessive amount of operability margin to accommodate transient operability at the expense of efficiency and performance. In addition, TEEM provides the ability to tailor the transient response of an engine, which could provide a number of other benefits.

TEEM has relevancy to many of the National Aeronautics and Space Administration (NASA) hybrid-electric aircraft concepts. NASA has developed a number of hybrid-electric fixed-wing aircraft concepts and vertical lift vehicles that include electrified turbomachinery through the use of an EM on one or more of the engine shafts. Given that these concepts possess most or all of the components necessary for implementing TEEM, the drawbacks for implementation are relatively small. However, the TEEM technology is not limited to application on futuristic hybrid-electric concepts. It is believed that TEEM could have the potential to buy its way onto conventional gas turbine engines in the near term. Application of TEEM to conventional turbofan engines could be an early step in the adoption of electrified propulsion that will help to accelerate the path toward more electrified and more efficient hybrid-electric concepts. To illustrate this point, this paper presents the application of the TEEM concept to an advanced turbofan engine model known as the Advanced Geared Turbofan 30,000 lb_f (AGTF30) (Ref. 9). This model represents a standalone turbofan engine that has been modified for this study to add EMs and supporting electrical hardware necessary to implement TEEM.

Prior work, presented in Reference 8, demonstrated the feasibility of the TEEM concept through simulation while being applied to the NASA conceptual parallel hybrid-electric turbofan (hFan) (Refs. 10 and 11). The ability to eliminate the stability bleed and suppress engine transients to reduce or even eliminate the operability margins allocated for handling transients was demonstrated through open-loop simulations. The previous work is extended here by developing control strategies and logic for implementing the TEEM concept. Three variant configurations of

the engine system are considered. These configurations are identified by the shafts that possess EMs. The dual-spool configuration has EMs on both spools, the high pressure spool (HPS) configuration has a single EM coupled to the HPS, and the low pressure spool (LPS) configuration has a single EM coupled to the LPS.

The paper is organized as follows. Section II summarizes details and observations about the TEEM technology made in Reference 8 that are relevant to the effort documented in this paper. Section III gives a brief overview of the AGTF30 model that serves as the platform for this study. Section IV describes the control aspects to implementing the TEEM concept in this application. Section V describes the control logic used to implement TEEM. Section VI presents simulation results that illustrate the proper operation of the controllers throughout the entire flight envelop. In addition, operation of the TEEM control logic is illustrated over an entire civil transport mission, and an example of transient performance is illustrated for a burst-and-chop transient scenario at sea level static (SLS) conditions. Finally, Section VII provides some concluding remarks.

II. TEEM Observation Review

Reference 8 demonstrated feasibility of the TEEM concept while being applied in simulation to the hFan engine model. The hFan engine model has a 1380 hp motor on the LPS and it was assumed to have a starter motor on the HPS. Results demonstrated that the function of the Low Pressure Compressor (LPC) stability bleed valve, otherwise known as a Variable Bleed Valve (VBV), could be replaced with power modulation on the engine shafts via EMs. To provide the same LPC stall margin maintained solely by the VBV, power extraction on the LPS and or power addition on the HPS is required. When it comes to implementation of the transient operability concept of TEEM, it was shown through simulation that the appropriate torque or power input on the shafts can keep an engine operating on its steady-state operating line. To achieve this, the torque inputs on the shafts were made such that the steady-state speed vs. fuel flow relationship was satisfied. This requires power addition on both spools during acceleration transients and power extraction on both spools during deceleration transients. However, it was discovered that power modulation is not required on both shafts simultaneously in order to achieve an operability benefit. Applying power to the HPS during acceleration transients and extracting power from the LPS during deceleration transients was sufficient to address the transient operability issues. Furthermore, it was found that the full amount of power required to maintain the steady-state operating lines was not necessary and could be substantially reduced without significantly impacting the operability benefits. It was determined that a 1200 hp EM on the LPS and a 200 hp EM on the HPS was sufficient to prevent significant stall margin undershoot during the engine transients. This is within the realm of capabilities for the LPS EM present in the hFan concept and an electric starter motor on the HPS. Knowledge gained from these studies has been leveraged in the development of controls for the application in this paper.

III. Overview of the AGTF30 Engine Model

The AGTF30 is a high bypass turbofan engine capable of producing 30,000 lb_f of thrust at SLS conditions. The AGTF30 engine model is coded in the MATLAB/Simulink environment and was developed using the Toolbox for Modeling and Analysis of Thermodynamic Systems (T-MATS) (Ref. 12). The AGTF30 was created to match the performance of the NASA N+3 reference engine implemented using Numerical Propulsion System Simulation (NPSS) code (Ref. 13). NASA N+3 implies that the engine is representative of technology expected to be available in the 2030 to 2035 timeframe. In this case, it features a geared turbofan, a compact gas turbine, and a Variable Area Fan Nozzle (VAFN). The AGTF30 is a 0-D dynamic model that utilizes performance maps to capture component performance. The engine model includes a realistically-performing full-flight envelope controller that was originally developed in Reference 9. It has an active fuel flow rate controller with limit logic and utilizes scheduled control logic for the VBV and VAFN. The engine also has Variable Stator Vanes (VSV) in the high pressure compressor (HPC). The nominal impact of the VSV is built into the HPC performance map. The engine components have health parameters that can be adjusted to capture the impact of degradation based on a model taken from the Commercial Modular Aero-Propulsion System Simulation 40,000 lb_f engine model (Ref. 14). A degradation variable is featured to adjust the health parameters to represent the continuous spectrum of engine health from new to end-of-life. Note that the TEEM controller development and analysis considers a mid-life engine. The baseline engine is traditional in the sense that it is not electrified. In other words, the baseline engine does not have any EMs or assume any other electrical components as part of the propulsion system. This study assumes the addition of one or more EMs along with energy storage devices (ESDs) and any other supporting electrical equipment.

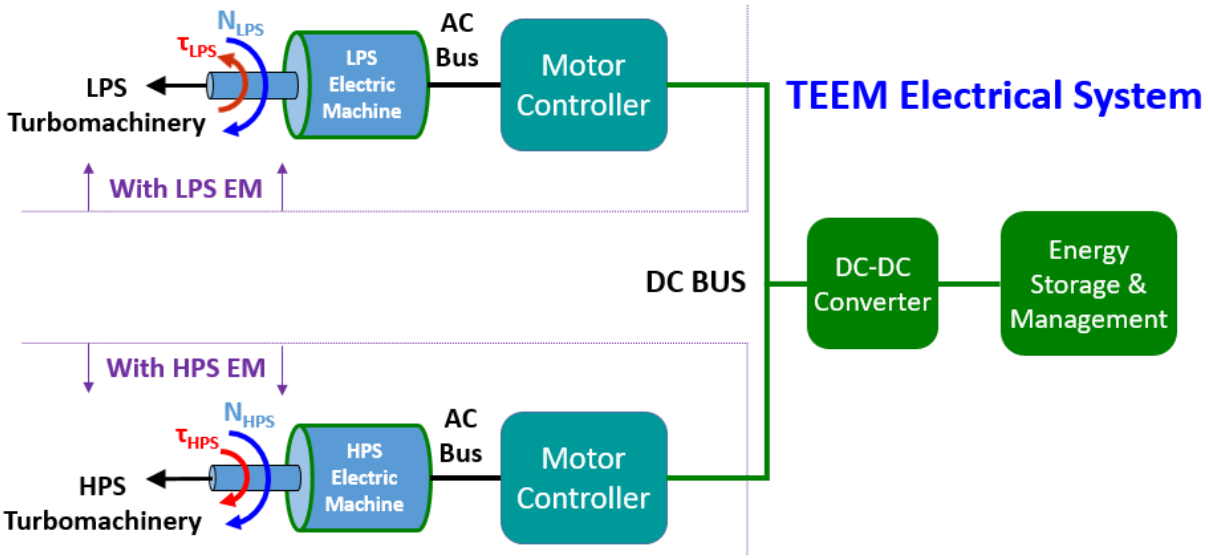

Figure 1.—Schematic of a proposed electrical system architecture for TEEM. Power addition is depicted for the HPS EM while power extraction is depicted for the LPS EM.

The electrical system is modeled using the Electrical Modeling and Thermal Analysis Toolbox (EMTAT). EMTAT is currently under development at the NASA Glenn Research Center and has evolved from the electrical system modeling effort documented in Reference 15. EMTAT is a Simulink library of electrical system components with a fidelity that is appropriate for capturing turbomachinery and electrical system interactions. Figure 1 is a high level schematic of a proposed architecture of the TEEM electrical system. The system consists of EMs coupled to one or both of the engine spools, a motor controller for each EM, a Direct Current to Direct Current (DC-DC) converter, and energy storage and management elements. In Figure 1, N_{LPS} and N_{HPS} are the speeds of the LPS and HPS, respectively. Similarly, τ_{LPS} and τ_{HPS} are the torques applied to the LPS and HPS by the EMs. Also note that AC is an abbreviation for alternating current. While the supply, extraction, and storage of energy necessary for implementing TEEM could be achieved in a variety of manners, the architecture considered here consists of one or more EMs, a super-capacitor bank, a DC-DC converter, motor controllers that include inverter and rectifier elements, and supply cables. The LPS configuration will also require a means of dissipating excess energy that is extracted from the spools during transient events but cannot be absorbed by the ESDs. Thus a bleed resistor bank is assumed to be present only in the LPS configuration. This architecture and its model parameters represent a notional power system intended to support the electric machines that enable the TEEM concept. It does not necessarily reflect the actual means of implementation, but instead offers a rough starting point for power system design that should be reconsidered and optimized in the future.

The electrical machines apply torque to the shafts for power addition or extraction. The inverters and rectifiers handle power conversions between DC and AC realms. The DC-DC converter regulates the voltage of the DC bus. The super-capacitor provides power to handle the impulsive power demands during transients. The resistor bank, which is only present in the LPS configuration, dissipates excess power that cannot be absorbed by the super-capacitors. Cables transmit power between electrical components. Note that it was beyond the scope of this effort to consider the management of heat produced by excess power extraction, or generated through inefficiencies of the electrical components. Table 1 summarizes the modeling parameters of the electrical system used in the application to the AGTF30 engine. The efficiency of the electrical machines were defined based on maps relating the efficiency to the torque and speed. Similarly, the efficiency of the DC-DC converter and the inverters/rectifiers were defined by maps relating the efficiency to voltage and current. The maps were produced from an empirical characterization of a model of the Subsonic Ultra Green Aircraft Research (SUGAR) Volt hFan power system as presented in Reference 16. The maps were scaled to match the defined system parameters. Refer to Reference 17 for details on the techniques used to model the electrical system.

TABLE 1.—BASIC PARAMETERS OF THEELECTRICAL SYSTEM MODEL

Component	Parameter	Value
Super-Capacitor	Equivalent Capacitance	86.4 F
	Equivalent Series Resistance	0.0031 Ω
	Leakage Current	0.04 Amps
	Maximum Voltage	500 V
DC-DC Converter	Bus Voltage	1000V
	Maximum Efficiency	0.98
Bleed Resistor Bank	Resistance	0.5 Ω
Power Supply Cable	Resistance	0.001 Ω
Motor Cables	Resistance	0.001 Ω
LPS EM	Maximum Torque	600 ft-lb_f
	Maximum Power	750 hp
	Maximum Speed	7500 rpm
	Maximum Efficiency	0.96
	Resistive Impedance	0.01 Ω
HPS EM	Maximum Torque	200 ft-lb_f
	Maximum Power	750 hp
	Maximum Speed	23000 rpm
	Maximum Efficiency	0.96
	Resistive Impedance	0.01 Ω
LPS EM Inverter and Rectifier	Voltage/Flux Constant	0.996 V/Hz
	Maximum Efficiency	0.98
HPS EM Inverter and Rectifier	Voltage/Flux Constant	0.307 V/Hz
	Maximum Efficiency	0.98

IV. TEEM Control Aspects

TEEM could be used to achieve a variety of goals. In this application, the effort in Reference 8 is built upon. TEEM is used to help address the low power operability problem and improve transient operability in order to enable more efficient engine designs. Energy storage is required to achieve these goals, so the ability to charge ESDs through use of the EMs is desirable. Therefore, three aspects of TEEM control are addressed: low power operability, charging, and transient operability. Each of these aspects will be discussed in the following sub-sections.

A. Low Power Operability

The VBV is a bleed valve, typically located immediately aft of the LPC, that is used to improve LPC operability. It is used to enable engine operation at low power conditions such as when the engine is idling or taxiing. As shown in Figure 2(a), the operability issue is the result of high incidence flow. The angle at which the air flow impinges on the blade is set forth by the incoming air flow drawn through the engine and the blades rotational speed. To simplify the visualization, the incoming flow velocity is drawn to be parallel with the axis of rotation of the engine. Left unaddressed, the high angle of attack could result in additional losses, and separation that can ultimately lead to compressor stall. The VBV solution bleeds air off of the back end of the LPC to allow more air to be drawn through it, thus increasing the incoming velocity and reducing the effective angle of attack. This solution is shown in Figure 2(b). This is a reluctant and inefficient solution as it requires compressed air flow to be bled from the core without any work extraction.

The presence of EMs enable another solution. This solution is to supply and or extract power on the engine shaft(s) to modify the rotational speed of the blades and/or alter the amount of air drawn through the compressor while allowing the amount of bleed through the VBV to be reduced. Applying power to the HPS will have the primary effect of increasing the flow rate through the core to increase the incoming flow velocity. Extracting power from the LPS will have the direct effect of reducing the rotational speed of the LPS. While this would improve the issue, the speed of the LPS does not actually change because it is directly coupled to the fan whose speed is being controlled by the fuel flow control loop. However, the extraction in LPS power prompts an increase in fuel flow which increases the speed of the HPS in order to maintain the desired fan speed. Thus power extraction on the LPS prompts power addition on the HPS, which increases the amount of air drawn through the LPC. In theory, bleeds, power extraction on the LPS, and power addition on the HPS, can be used independently or in combination to correct the flow condition. Such a solution is shown in Figure 2(c). Here the VBV area is reduced and power is extracted from the LPS and or added to the HPS. In these figures, blue lines are used to represent the impact of air bleeds while the impact of power extraction and addition are signified with a red line.

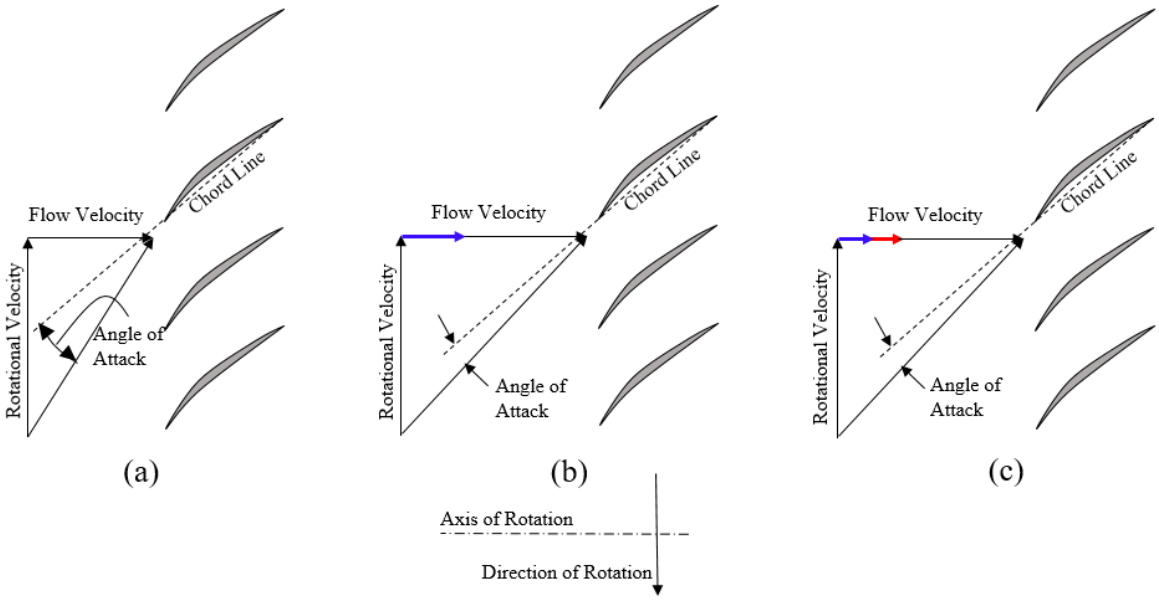

Figure 2.—Simplified LPC blade stage illustration and the impact of the VBV and power modulation on the shafts: (a) without bleeds or power modulation, (b) VBV solution, (c) combined VBV and power modulation solution.

Whereas the VBV solution dumps air into the bypass duct resulting in unrecoverable losses, power extraction on the LPS can be used to charge ESDs. While power extraction on the LPS will require a higher fuel burn for the same amount of thrust, it will also promote combustor stability. The improved combustor stability could allow the fuel burn to be reduced while the engine is operated at a lower thrust level than can be achieved by the baseline engine. Assuming the minimum fan speed is not limited by other operational limits, this could be advantageous when the engine is idling on the ground and the ESDs are not fully charged. A drawback to power extraction from the LPS is that it may reduce the fan stall margin as is the case for the AGTF30. Since the AGTF30 has a VAFN, this issue can be remedied by increasing the VAFN area. As a result, the VAFN schedule and maximum VAFN area may need to be re-considered.

Power addition on the HPS will have the benefit of reducing the fuel burn for the same amount of thrust. This solution also tends to increase the fan stall margin and reduce the maximum area required by the VAFN to maintain operability. If the power input on the shaft is simply a reduction of power extraction from the HPS, which is typically present to power aircraft systems, then the fuel savings are only offset with the penalty of reduced aircraft power while this approach is applied. In this event, it may be necessary for power to be cut or limited for non-essential aircraft systems. While this is likely to be undesirable in-flight, it could be an option during ground operations. However, reduction in power extraction from the HPS will be limited by how much power the aircraft can afford to give up. If the aircraft is already operating with minimal power, this strategy will not be applicable. Another option is to provide power or supplement reduced power extraction on the HPS using the ESDs. If the energy is more efficiently acquired and applied by the ESDs than by burning fuel at the current power setting, then using ESDs to supply power is advantageous. For example, if the power supplied by the ESDs was extracted from the engine while it was operating at a more efficient operating point, or if the energy in the ESD originated from the grid at a lower overall cost, then supplying power using ESDs could be advantageous. Though, the use of ESDs in this manner would have limitations. The energy in impulsive energy storage elements, such as super-capacitors, should be conserved to address transients, particularly during take-off. It may be possible to make dual-use of onboard ESDs, such as those used for starting aircraft systems and the auxiliary power unit (APU). Still, the energy capacity and power would be limited, which could constrain use of the HPS power input for this purpose. Thus, HPS power input may be best suited for select operating modes such as during ground operations. Whatever the case may be, the system would need to be sized to account for the potential usage of energy stored in the ESDs.

B. Charging

The application of the transient TEEM concept during acceleration transients is dependent on the addition of power, which implies the use of ESDs. The ability to re-charge ESDs in-flight will help to minimize their size and promote efficient turn-around times for the aircraft. Furthermore, the ability to re-charge in-flight will help to minimize the services that must be performed on the ground to charge or replace the ESDs, as well as the infrastructure required to support these services.

Through simulation analysis it was observed that power extraction from the LPS required less of an increase in fuel flow to maintain the desired corrected fan speed. Since it is more efficient to extract power directly from the LPS, the LPS EM will be used for power extraction to charge the ESDs, if the configuration has an LPS EM. If an EM only exists on the HPS, there will be no choice but to extract power from the HPS for charging.

The amount of power extraction will likely be dependent on the maximum charge rate of the ESDs, a practical maximum area limit of the VAFN, or a practical limit on the power that can be extracted from the given engine spool without significantly degrading performance or operability. At low power, the VBV and VAFN should be coordinated with power extraction to maintain operability. At high power, the operability of the LPC and fan improve making power extraction for charging less of a concern. However, at very high power conditions, power extraction can reduce the maximum thrust and cause some control limits, such as the over-temperature limit, to be reached sooner. Therefore, one may consider limiting power extraction at these conditions. Also, the AGTF30 was observed to require an additional limitation on the power extraction from the HPS at very high altitudes. Near the very top of the flight envelope, the engine's HPC SM significantly decreases. Power extraction, particularly from the HPS, has the tendency to decrease HPC SM. This worsens the situation and could potentially result in a violation of the minimum acceptable HPC SM while operating in steady-state or upon an acceleration transient. If not considered when implementing TEEM, it could cause the HPC to stall.

Given that the energy storage in the proposed architecture consists of only super-capacitors that are meant to supply and absorb impulsive loads, the super-capacitors are not expected to place any limitation on a practical amount of power extraction for charging. Instead, the amount of power extraction is expected to be driven by the desired super-capacitor charge time as well as turbofan performance and operability considerations.

C. Transient Operability

The transient operability improvements enabled by TEEM expand the design space of the engine to enable more efficient designs. Active modulation of the power addition/extraction on the shafts can reduce or even eliminate the operability margins allocated for transient operation. Assuming and EM is present on both spools, based on prior work (Ref. 8), it is expected that power addition on the HPS will increase HPC SM during accelerations while power extraction on the LPS will increase LPC SM during decelerations. As we consider the use of a single EM on a single shaft, it was hypothesized that power addition on the HPS could increase LPC stall margin during decelerations and power addition on the LPS could help to increase HPC stall margin during accelerations.

The quick responsiveness of EMs enables them to shape and tailor the transient to a large degree. This can simplify control design for the fuel control loop, especially when it comes to acceleration and deceleration logic. Acceleration and deceleration logic is put in place to prevent the fuel controller from commanding too much or too little fuel during transients such that it could jeopardize operability. Since the EMs now handle the operability issue, the job of the fuel control acceleration and deceleration logic is to ensure that any commanded fuel flow rate does not demand too much effort from the EMs. The following section includes a discussion regarding simplification of the control logic.

There is also a control aspect to the use or dissipation of excess energy when power is extracted during transients. This applies to the dual spool and LPS configurations in which power is extracted from the LPS during deceleration transients. During such an event, the amount of power extracted from the LPS will likely exceed what can be absorbed by the ESDs. Whatever power cannot be absorbed by ESDs must be immediately used or dissipated. The dual-spool configuration immediately applies the excess power extracted with the LPS EM to the HPS via the HPS EM. This approach further promotes LPC operability and avoids the need to dissipate excessive power. The LPS configuration does not have an HPS EM to expend the excess power. Therefore, the excess power is dissipated in a bleed resistor bank. Both techniques require some associated control logic.

V. Control Logic

Low power operability, charging, and transient operability goals must be coordinated to simultaneously maintain operability while improving or preserving performance during application of the TEEM concept. To address this, logic is used to determine when and how the EMs are used to achieve the goals. Note that while there may be merit to applying power addition on the HPS during certain segments of steady-state operation, it was not the main focus of this effort and was not implemented in the control strategy presented here.

During a transient, priority will be given to addressing the transient operability issue. Low power operability during a transient will be handled solely by the VBV. Any charging of ESDs, other than through power extraction meant to improve transient operability, will cease in order to preserve responsiveness. During decelerations, extracted energy can be utilized to charge the ESDs if they are not already sufficiently charged. However, in the event that the ESDs are fully changed, that energy will be used or dissipated immediately via the HPS EM or a bleed resistor bank.

During steady-state operation while the ESDs are sufficiently charged, low power operability will be handled by the VBV. When operating in steady-state while the ESDs are not sufficiently charged, the EMs may be used as generators to charge the ESDs. The manner in which low power operability and charging is managed will be dependent on the configuration of the system. If an EM exists on the LPS then that EM will be used for charging. Otherwise, the HPS EM will be used. Power extraction will need to be coordinated with the VBV and VAFN to maintain LPC and fan operability. Therefore, the VBV and VAFN schedules must be modified.

A high level view of the controller structure is provided in Figure 3. The TEEM control logic introduces active torque controllers for the EMs, scheduled logic for charging, and activation/de-activation logic. Feedback from the power system is also used to modify the VBV and VAFN schedules. The fuel flow controller also contains simplified acceleration and deceleration schedules as will be discussed later. A high level representation of the control approach is shown in Figure 4 to Figure 6 for the dual-spool, HPS, and LPS configurations, respectively. The blue blocks indicate some high-level control decisions while the white boxes indicate decision making criteria. The controller components and their control logic will be discussed in more detail in the following sub-sections.

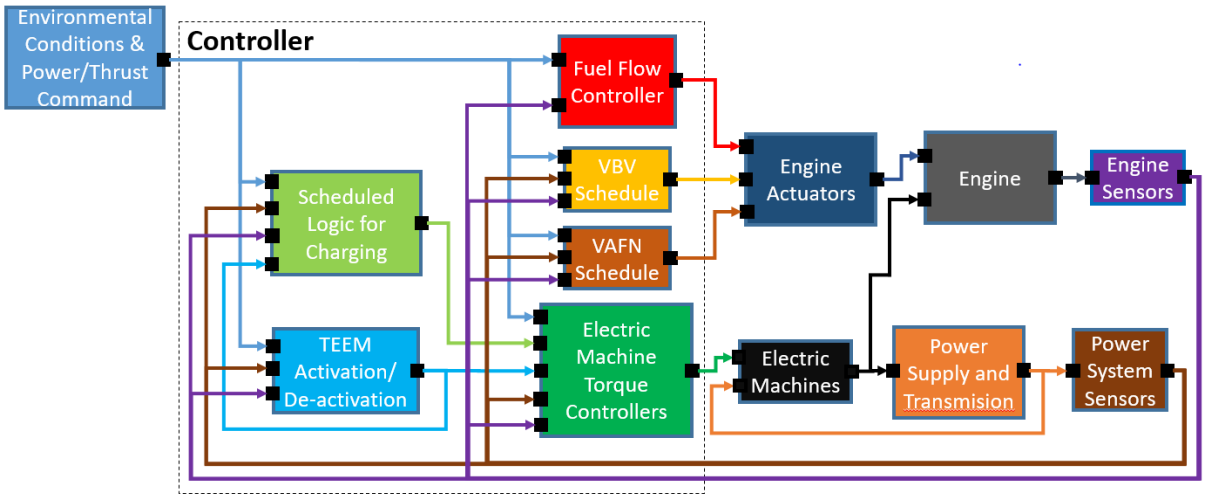

Figure 3.—High level representation of the overall control structure.

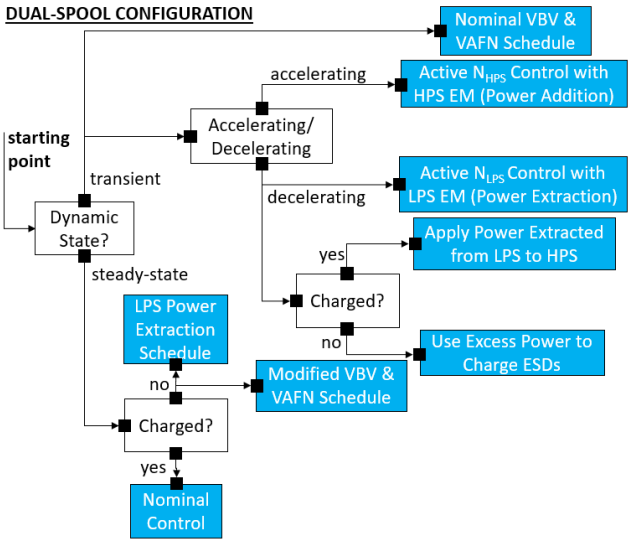

Figure 4.—High level control logic for the dual-spool configuration.

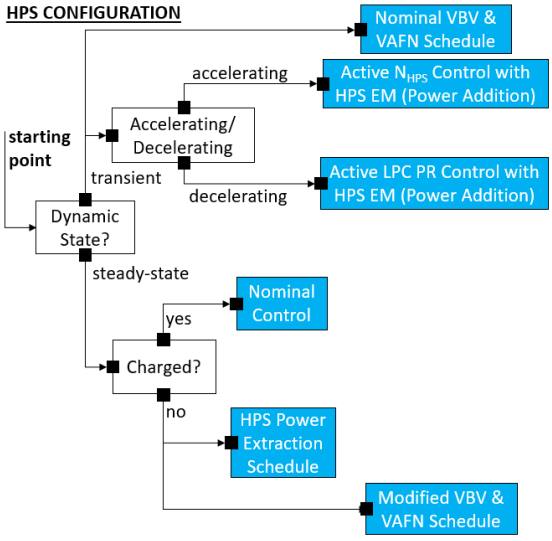

Figure 5.—High level control logic for the HPS configuration.

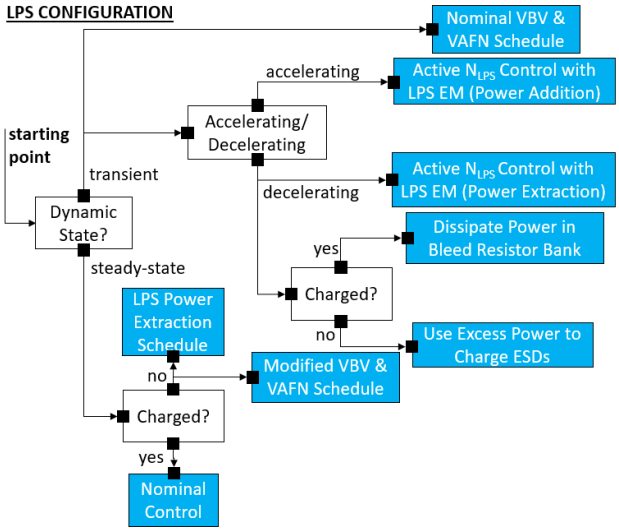

Figure 6.—High level control logic for the LPS configuration.

A. The Low Power Operability Problem and Charging

The control solution to the low power operability problem and charging will be discussed at the same time because they are handled simultaneously. During steady-state operation, the only off-nominal use of the EMs is to charge the ESDs. While the shaft power is altered, the VBV and VAFN are coordinated with the off-nominal EM torque input to maintain the same level of operability present in the baseline engine.

The amount of power extraction from either shaft is set by a schedule. In the case of charging the super-capacitors, the power extraction is scheduled based on the super-capacitors normalized voltage which is defined by Equation (1) where V_n is the normalized voltage, V_{SC} is the voltage across the super-capacitor bank, and $V_{SC,max}$ is the voltage at which the super-capacitor bank is considered to be at full charge. Note that the $V_{SC,max}$ value may differ from the absolute maximum voltage of the super-capacitor bank.

$$V_n = \frac{V_{SC}}{V_{SC,max}} \tag{1}$$

In the application to the AGTF30 engine, the scheduled power extraction, P_{sched}, is 75 hp for most conditions but begins to taper off toward zero once V_n exceeds 0.97. This is done to help prevent over charging the super-capacitors. For this application, the super-capacitor bank is considered to be fully charged once V_n reaches 0.989. The power extraction command is altered by two power modifiers, F_{VHEP} and F_{VHA}, which reduce the power extraction at very high engine power and very high altitude, respectively. The commanded power extraction, P_C, is given by Equation (2).

$$P_C = P_{sched} F_{VHEP} F_{VHA} \tag{2}$$

The power modifiers prevent the power extraction from impacting peak performance and help to preserve a high degree of operability at very high altitude. F_{VHEP} is scheduled based on the Power Lever Angle (PLA) which refers to the position of the engine's throttle. It correlates to the power/thrust demand from the engine. For the application to the AGTF30 engine, the PLA range is between 40° and 80°, with 40° corresponding to ground idle and 80° corresponding to maximum thrust/power. The F_{VHEP} schedule was set to taper off to zero at high PLA values that are above the power settings at which the engine should be continuously operated. F_{VHA} is scheduled based on altitude. The schedule was created after observing the results of numerous simulations conducted at altitude in order to determine how the steady-state SMs are impacted as altitude increases. Some tuning was conducted to select the values of F_{VHA}. In general, the values of F_{VHA} gradually taper to zero at high altitudes in order to prevent the SM from being reduced while charging at flight conditions that lack significant operability margin. Plots of the schedules are shown in Figure 7. The torque command is calculated using P_C and the sensed speed of the appropriate shaft.

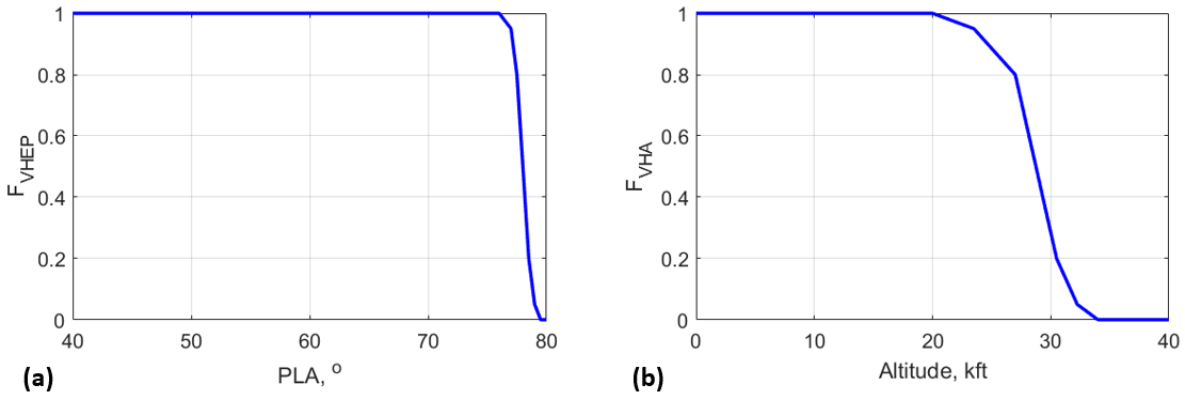

Figure 7.—F_{VHEP} (a) and F_{VHA} (b) schedules.

To maintain LPC and fan operability, the VBV and VAFN schedules, which are stored in two-dimensional lookup tables based on Mach number and corrected fan speed, are appended to include off-nominal torque modulation on each applicable spool as an additional dimension for interpolation. Since off-nominal torques will not be applied on both spools at the same time, two separate three-dimensional schedules may be used in place of a single four-dimensional schedule. To construct the new schedules, simulations were run throughout the flight envelop for various power conditions and amounts of applied torque. During these simulations, the VBV and VAFN were actively controlled to achieve the same LPC SM and fan SM as the baseline model. The VBV and VAFN values were recorded and later used in the construction of the new schedules. The deviations from the nominal schedules are modest. The maximum VBV area remains unchanged and the maximum VAFN area is increased by less than 2%, and only when using an EM on the LPS. The deviations are the most significant at low power and low Mach numbers.

B. Transient Operability

During engine transients, a goal of the control logic is to prevent excessive reduction in the operability limits. Specifically, the reduction or elimination of HPC SM undershoot during accelerations, and LPC SM undershoot during decelerations. Reference 8 revealed that this could be achieved by applying TEEM to maintain steady-state shaft speed vs. fuel flow relationship(s). Therefore, one TEEM-based control approach is to implement speed control on the shafts to maintain these relationship(s). The set-point shaft speeds are scheduled based on Mach number, altitude, and normalized fuel flow. The normalized fuel flow is given by Equation (3).

$$w_{f,norm} = \frac{w_{f,sen} - w_{f,min}}{w_{f,max} - w_{f,min}} \tag{3}$$

In Equation (3), the maximum and minimum fuel flow rates at the current Mach number and altitude are given by $w_{f,max}$ and $w_{f,min}$, while $w_{f,sen}$ is the sensed fuel flow. The set-point speed schedules were produced by running various simulations throughout the flight envelope at different power conditions. While fuel flow measurements are known to suffer from inaccuracies, it will be shown that the performance of the controller is not effected significantly by practical levels of measurement error. In an effort to reduce the impact of fuel flow bias, the fuel flow measurement is artificially compensated. By imposing a positive compensation bias on the fuel flow signal while accelerating, it will demand slightly more power from the HPS EM. This should improve the HPC SM further. By imposing a negative compensation bias on the fuel flow signal while decelerating, it will demand more power from the HPS EM or more power extraction with the LPS EM. Either way, the compensation should be beneficial to the LPC SM during decelerations. Also note that the estimation of fuel flow bias is possible through the use of techniques such as Kalman filters or optimal tuner Kalman filters (Ref. 18).

In the dual-spool configuration, speed control is a promising approach for achieving the goal of improved operability of both shafts. The speed of the HPS will be the control variable for the HPS EM during accelerations while the LPS EM is not used. The speed of the LPS will be the control variable for the LPS EM during decelerations. In the dual-spool configuration, the HPS EM will be used during decelerations but only to apply excess power extracted by the LPS EM. As the normalized voltage of the super-capacitor approaches 1 (full charge), the HPS EM will be commanded to apply a fraction, F_C, of power extracted from the LPS based on the schedule in Figure 8. As V_n approaches 1, the amount of power applied to the HPS by the HPS EM increases until it matches the power extraction from the LPS.

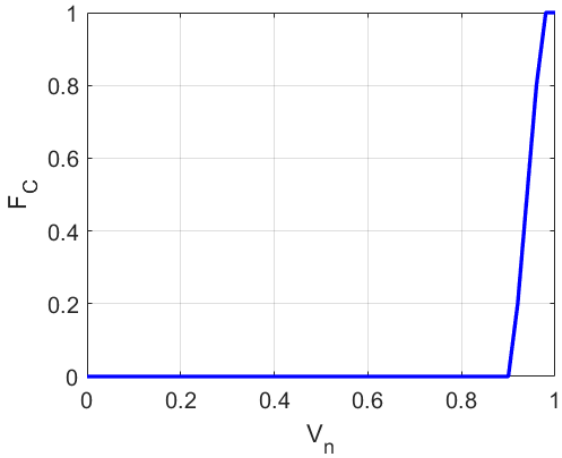

Figure 8.—Fraction of the power extracted by the LPS EM that is applied to the HPS EM during decelerations.

In the LPS configuration, the speed of the LPS will be the control variable for the LPS EM during both accelerations and decelerations. Any excess power extracted during deceleration transients will be dissipated in the bleed resistor bank.

In the HPS configuration, speed control is applicable for improving the HPC SM during accelerations, but it is not applicable during decelerations because the set-point schedule would call for power extraction on the HPS that would exacerbate the LPC SM issue. To correct the deceleration LPC SM issue, torque should be applied to the HPS. Therefore, a different control strategy is necessary. Perhaps the most direct approach is to control the LPC SM, which would require an estimator or some sort of advanced model-based control. To make the control more amenable to modern control and sensing methods, a LPC pressure ratio (PR) controller is implemented. Note that a LPC discharge pressure controller may also be applicable. Similar to the speed set-points, the LPC PR set-point schedule is a function of Mach number, altitude, and the normalized fuel flow rate. The LPC PR set-point schedule was created in the same manner as the speed set-point schedules.

Active control of the EM(s) is performed with gain scheduled Proportional Integral (PI) controllers. The control gains are interpolated based on the Mach number, altitude, and PLA. It is not desirable for the transient control logic to remain active during steady-state operations as it could alter steady-state performance and result in the unnecessary and wasteful use of stored energy and or the unnecessary dissipation of energy in the form of heat. Thus, activation logic is utilized to prevent this from occurring. Furthermore, logic is applied so that the EMs are only used when they are the most beneficial.

Activation/de-activation logic uses the normalized error, $\bar{e}$, to help determine when the transient controllers should be applied. The normalized error is defined as the error in the current active fuel flow control variable normalized by the expected range in variation of that control variable. The term “active fuel flow control variable” is referring to the variable that is being regulated by the fuel flow control loop. In the case of the AGTF30 engine, this will either be the fan speed, or one of the limit variables such as the inter-turbine gas temperature. As an example, if the nominal corrected fan speed controller is active, the set-point command is 6000 rpm, the sensed corrected speed is 5500 rpm, and the expected range in corrected speed variation is 5000 rpm, then the normalized error is (6000 – 5500)/5000 = 0.1. Note that the control variable used to calculate the normalized error may change as the active fuel flow controller changes. This may occur when certain limits are approached such as those set by acceleration, over-speed, and over-temperature limit logic. The sign and magnitude of the normalized error is used to determine if the engine is accelerating, decelerating, or in steady-state and this information will be used to activate or de-activate certain control elements. If the magnitude of the error is above a defined threshold then the engine is assumed to be going through a transient. In this application, the threshold was selected to be 0.025. If the normalized error is positive then the engine is accelerating. If it is negative then the engine is decelerating. Recall that if an EM exists on the HPS, that EM will be used during accelerations. During decelerations the LPS EM will be active if one exists, otherwise the HPS EM will be used.

Some care was taken with transitioning the controller from active to inactive. This was done by introducing a transition factor, *C*, that is multiplied by the torque command generated by the PI controller to form the command that is sent to the electric machine. This tapers the torque command to zero as the normalized error approaches zero. *C* is given by the logistic function:

$$C = \frac{1}{1 + e^{-k(\bar{e} - \bar{e}_o)}} \tag{4}$$

where $\bar{e}_o$ and k are defined below.

$$\bar{e}_o = \frac{1}{2}(\bar{e}_L + \bar{e}_U)$$

$$k = \frac{-\ln(99)}{\bar{e}_L - \bar{e}_o}$$

$\bar{e}_L$ *and* $\bar{e}_U$ are the lower and upper normalized error values at which *C* is within 1% of 0 and 1, respectively. In all cases, these values were 0.025 and 0.05, respectively. This means that the commanded torque will begin to reduce to zero once the normalized error reduces to 5% and will essentially be zero for any error below 2.5%, for which the controller should be inactive.

In the special consideration of the LPC PR controller for the HPS EM in the HPS configuration, the LPC PR set-point is artificially altered during transients to further improve the LPC SM. The set-point command is multiplied by a modifier, *m*, which is defined by a logistic function in a similar manner to *C*. This is done in order to make the set-point LPC PR slightly lower than the scheduled value.

$$m = \frac{X - 1}{1 + e^{-k(\bar{e} - \bar{e}_o)}} + 1 \tag{5}$$

The difference from Equation (4) is that the logistic function shown in Equation (5) will be 1 when the normalized error is small and *X* when the normalized error is large. *X* is some positive value that is slightly less than 1 and can be adjusted to effect the operability benefit.

Another aspect of the transient TEEM controller is that it enables a simpler approach to acceleration and deceleration limit logic. Since the EM(s) manage the transient response to maintain engine operability, it alleviates that responsibility from the fuel controller. Typically fuel controllers have complex acceleration and deceleration schedules to limit the fuel flow rate in order to protect against violation of operability limits. Of particular concern is compressor stall. In the case of the AGTF30 engine model, it is equipped with acceleration and deceleration schedules that limit the fuel flow to prevent it from exceeding some maximum or minimum fuel flow to high pressure compressor static discharge pressure ratio, w_f/ps3. The acceleration controller for the AGTF30 engine determines the w_f/ps3 set-point via a 1-D look-up table based on corrected fan speed, whose output is modified based on altitude. Note that creation of the look-up table and altitude scaling factor required numerous simulations to be run in order to characterize the engines steady-state and dynamic performance, as well as some tuning to achieve the desired thrust responses. The fuel flow command is obtained by multiplying the set-point w_f/ps3 by the sensed ps3. For some applications, acceleration and deceleration schedules may require multi-dimensional look-up tables and more complex logic. For instance, the acceleration schedules designed in Reference 19 are three-dimensional look-up tables based on Mach number, altitude, and corrected fan speed. Some acceleration and deceleration controllers use the acceleration or deceleration of a shaft as the control variable. This approach not only requires a set-point schedule, but also the development of active feedback control laws. In any case, the acceleration and deceleration controllers will require studies be conducted to characterize the engine's steady-state and dynamic performance.

Since the EM(s) are now responsible for maintaining transient operability, the role of the fuel controller's acceleration and deceleration schedules is to limit the fuel flow such that quick changes in fuel flow do not demand more power than the EM(s) are capable of providing. This can simplify the design of the acceleration and deceleration schedules. To illustrate this, the rate of change in fuel flow was directly limited to achieve an approximate thrust response time. The change in fuel flow command during a time-step of the controller was set to not exceed a value that is consistent with achieving a desired thrust response time while applying a ramp input in fuel flow. The maximum deviation in fuel flow from the previous command is determined by Equations (6) and (7) for an acceleration and deceleration, respectively.

$$\Delta w_{f,accel} = \frac{w_{f,max} - w_{f,min}}{t_{r,approx}} t_s \frac{PLA - PLA_{min}}{PLA_{max} - PLA_{min}} \quad (6)$$

$$\Delta w_{f,decel} = \frac{w_{f,max} - w_{f,min}}{t_{r,approx}} t_s \frac{PLA - PLA_{max}}{PLA_{max} - PLA_{min}} \quad (7)$$

In these equations, t_s is the controller time-step and $t_{r,approx}$ is an approximate thrust response time. Due to shaft inertias, the actual response time may be slightly longer. The value of $t_{r,approx}$ will be different during acceleration and deceleration transients. In this case, $t_{r,approx}$ was scheduled based on the Mach number and altitude. PLA_{min} is the minimum *PLA* setting while PLA_{max} is the maximum *PLA* setting. Recall that the PLA position ranges from 40° to 80° for the AGTF30. However, PLA_{min} used in the calculation for the acceleration limit was 39°, and PLA_{max} used in the calculation of the deceleration limit was 81°. The reason for this was to avoid a case in which the maximum change in fuel flow command could be zero. In such a case, the limit controller may not allow the controller to change fuel flow commands and the engine could become stuck at its current operating condition. The reason for the inclusion of PLA in these calculations is to reduce SM undershoot in response to intermediate changes in power. While SM undershoot is nearly or completely eliminated at most operating points for an idle to full power or full power to idle transient, more SM undershoot was observed with and without TEEM implementation when intermediate power changes were made. During intermediate changes in power, the SM may undershoot the next steady-state value. This may occur because the difference in steady-state SM for near-by power settings can be small, providing less of an opportunity to correct the operability issue before undershooting the next steady-state SM value. Furthermore, the time of the transient is naturally shorter, giving the EMs less time to fix the issue before the minimum SM is encountered. Despite the undershoot in SM, the minimum SM reached during an intermediate power change is not likely to exceed the minimum SM experienced during an abrupt idle to full throttle or full throttle to idle transient. For that reason, this portion of the control logic may be unnecessary. However, it is implemented in the studies presented in the next section. The effect of this portion of control logic is to slow down the transient response in order to improve operability. The result will be a similar thrust response time, regardless of how much the power level changes.

In the proposed acceleration and deceleration limit logic, $w_{f,max}$ and $w_{f,min}$ are already determined by the TEEM control logic. Thus, the only thing that needs to be designed for the acceleration and deceleration limiters are the schedules for $t_{r,approx}$. The values of $t_{r,approx}$ are prescribed to get the desired thrust response and are approximately equal to the response time that is desired. Therefore the schedule can be created intuitively without performing extensive simulations and testing to characterize the engines performance and dynamics. Furthermore, these limit controllers are expected to be very similar for different engines, allowing for the schedules to be applied generically to multiple engine designs or easily adapted from one engine design to another. Benefits to the new acceleration schedule include simplification of the acceleration and deceleration limit logic and its design, a more direct prescription of the thrust response time, and consistency in the transient response of the engine despite degradation. Note that in the analysis to follow, the baseline model continued to use the w_f/ps3 acceleration schedule that was originally used by the model.

In the LPS configuration, power extraction during a deceleration could exceed the energy storage capacity of the super-capacitors and there is no HPS EM present to apply excess power. In this event, the excess energy must be dissipated. Thus, the bleed resistor bank is switched into the power system when the super-capacitor voltage approaches full charge. For the AGTF30 application, this occurred when the super-capacitor reached 99% of its maximum desired voltage. Note that the absolute maximum voltage of the super-capacitor bank will be higher than this value for safe measure. The equivalent resistance of the resistor bank is low enough that it will absorb the load from the EMs and slowly discharge the super-capacitors. Once active, the switch will remain closed until the super-capacitor voltage drops below a prescribed voltage in order prevent the resistor bank switch from rapidly changing between the open and closed positions. For the AGTF30 application, this was considered to be 97% of the maximum desired voltage.

VI. Simulation Results

The following sub-section illustrates the impact of TEEM and its controllers on the operability and performance of the AGTF30 engine. Baseline results refer to the stand alone engine model with its original controller and without EMs or any supporting electrical equipment that is associated with the implementation of TEEM. The first study evaluates a burst and chop transient at SLS conditions. The second study is a Monte Carlo analysis of the operability improvements achieved by the TEEM concept. The third study involves a full flight simulation that utilizes flight data to show the impact for a typical commercial transport mission. For each case, the three previously mentioned TEEM configurations are considered.

A. SLS Burst and Chop Transients

The model was run with an aggressive burst and chop transient profile at SLS conditions. This mimics an aggressive take-off scenario followed by an aggressive reduction in thrust. The engine starts at idle, the PLA is increased to its maximum position over the course of 1 s, and the maximum position is held for some time to allow the transient to settle out. The PLA is then decreased back to the idle position over the course of 1 s and some time is allowed for the transient to settle out. The thrust responses for the baseline control and the three different variants of the TEEM concept are shown in Figure 9. All three TEEM implementation variants, which apply the simplified acceleration schedule, are seen to provide a similar thrust response to the baseline engine control that satisfies the FAA requirement for thrust responsiveness (Ref. 20). The operability of the HPC and LPC are quantified using the stall margin metric as plotted in Figure 10(a) and (b), respectively.

A substantial ~4% HPC SM improvement is observed for the dual-spool and HPS configurations during accelerations while only a modest HPC SM improvement of ~0.6% is present for the LPS configuration. For the LPS configuration, there is also an undesirable reduction in LPC SM of over 2% during the acceleration transient. For the HPS configuration, there is a slight decrease in the HPC SM when the engine is at idle following the transients. This is a result of power extraction from the HPS in order to charge the super-capacitors. Once the super-capacitors are charged, the HPC SM returns to its nominal value. In theory, the VSV schedule could be adjusted to improve the HPC SM during this mode of operation. However, given that the HPC SM is already large at this condition, some reduction is viewed to be acceptable.

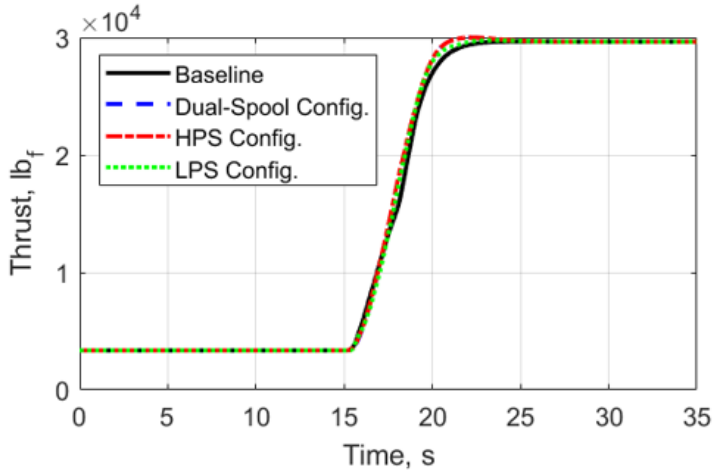

Figure 9.—Thrust response to and idle to full power throttle command.

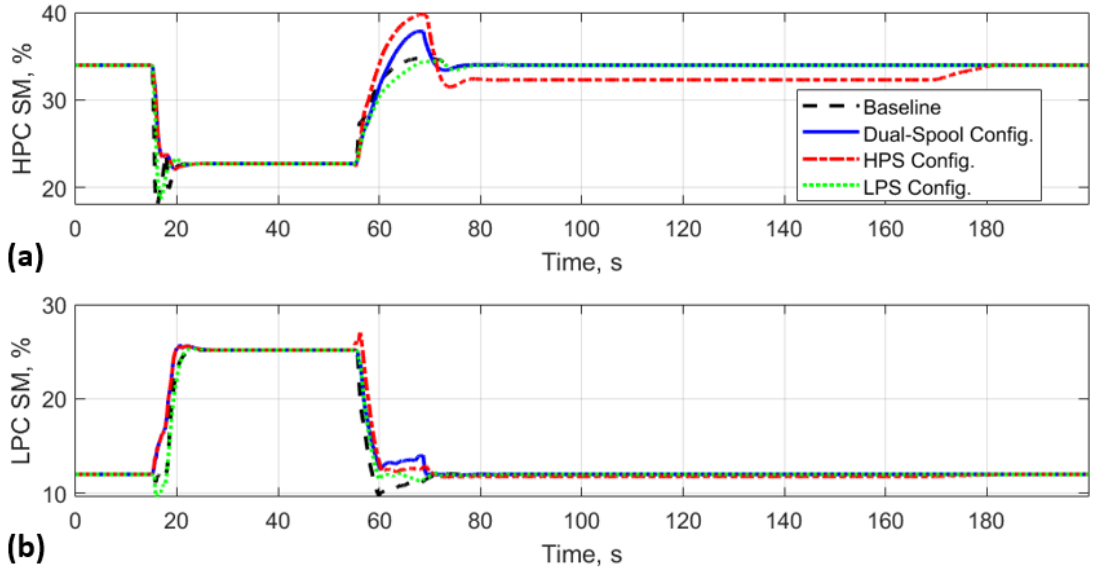

Figure 10.—HPC SM (a) and LPC SM (b) during an SLS burst and chop transient.

During the deceleration, a 2.2%, 2%, and 1.4% improvement in LPC SM is obtained with the dual-spool, HPS, and LPS configurations, respectively. Also notice that, despite off-nominal torque input on the shafts during portions of steady-state operation, the steady-state LPC SM is the same in all cases, indicating that the VBV schedule has been coordinated appropriately with the use of the EMs. The torques and powers applied to the shafts to achieve these results are shown in Figure 11. The total energy supplied by the super-capacitor and its normalized voltage are plotted in Figure 12. Less than 0.7 kW-hr of energy was supplied by the super-capacitors during the extreme acceleration transient. In the HPS configuration, the super-capacitor supplies an additional ~1.4 kW-hr of energy during the extreme deceleration transient. In the dual-spool and LPS configurations, power extraction during the deceleration charges the super-capacitors with 0.55 to 0.59 kW-hr of energy, respectively. This nearly recharges the super-capacitors in the dual-spool configuration leaving only 0.13 kW-hr of energy to be restored after the transient. Power extraction during the deceleration transient completely recharges the super-capacitors in the LPS configuration. The super-capacitors reach full charge during the transient and the resistor bank engages 3 times to dissipate the excess power. The 3 slight decreases in super-capacitor state of charge between 60 s and 75 s in Figure 12, corresponds to the activation of the resistor bank to bleed energy and keep the super-capacitor bank from exceeding its desired maximum voltage. The amount of energy dissipated (or heat generated) by the resistor bank is ~0.69 kW-hr.

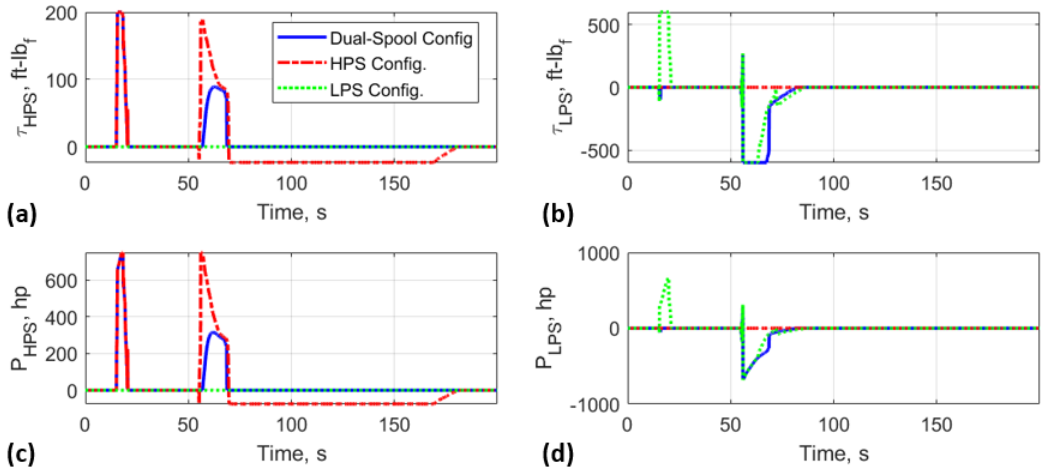

Figure 11.—Electric machine torque and power inputs for each configuration. HPS torque and power are shown in (a) and (c), respectively. LPS torque and power are shown in (b) and (d), respectively.

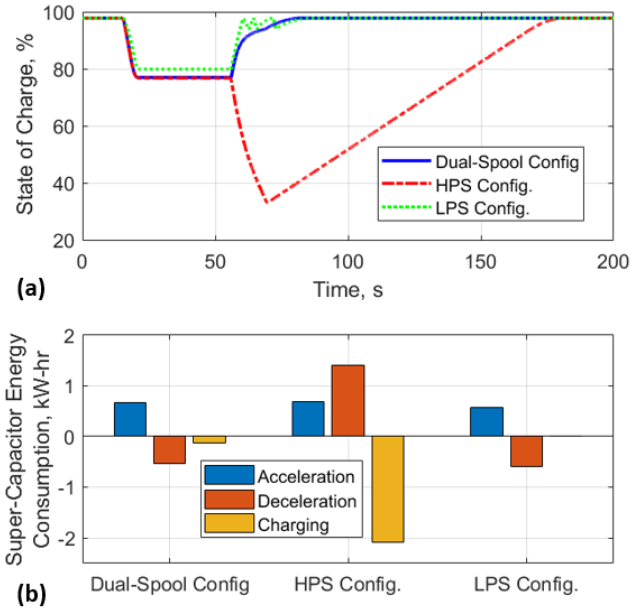

Figure 12.—Super-capacitor state of charge (a) and energy usage (b).

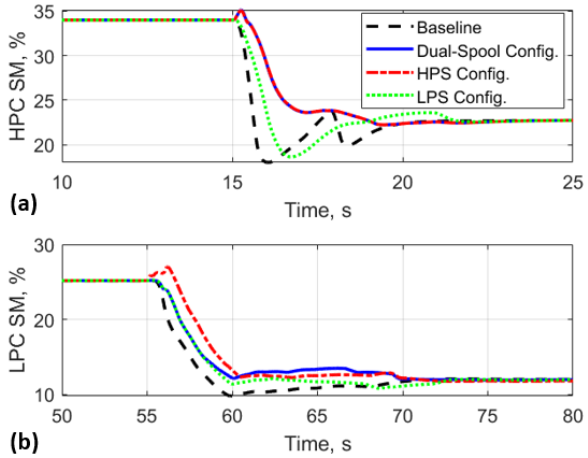

Figure 13.—HPC SM (a) and LPC SM (b) with a positive fuel flow bias.

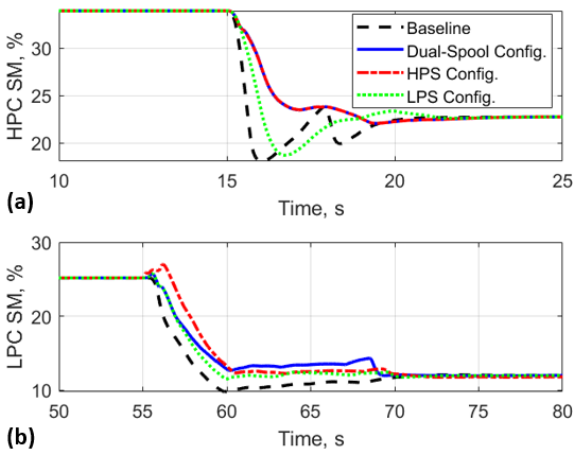

Figure 14.—HPC SM (a) and LPC SM (b) with a negative fuel flow bias.

While the dual-spool and LPS configurations take advantage of power extraction during decelerations to charge the super-capacitors, the HPS configuration does not. Furthermore, the HPS configuration requires more power addition during decelerations. Since the super-capacitors can only charge during steady-state operation in this configuration, it increases the time to charge and may increase the size of the super-capacitor in order to handle subsequent acceleration and decelerations transients. While the dual-spool and LPS configurations are nearly or fully charged after the deceleration transient, it takes roughly 100 sec to fully restore charge to the super-capacitors in the HPS configuration. Note that charging does not occur from 20 to 55 sec in any configuration because the engine is at maximum power and the control logic dictates that there be no power extraction at this condition in order to avoid degrading the engine's peak performance.

As mentioned previously, the TEEM controller utilizes the fuel flow rate measurement in the active control of the EMs. Since the fuel flow measurement can be inaccurate, it is of interest to see how an erroneous fuel flow measurement could alter the performance of the TEEM controller. Thus a fuel flow bias was applied in simulation to increase or decrease the sensed fuel flow by 2% of the current fuel flow or 0.5% of the maximum fuel flow, whichever is greater. The LPC and HPC SM are shown in Figure 13 for when the sensed fuel flow is above the actual value, and Figure 14 shows the results for when the sensed fuel flow is below the actual value. As can be seen, the fuel flow bias does not have a significant effect on the ability of the TEEM controller to improve the operability of the engine. This is evident in Figure 13 and Figure 14, which show that the SM undershoot was essentially eliminated during the transients despite the presence of fuel flow bias. The only exception is the HPC SM during the acceleration transient for the LPS configuration. It was noted earlier that the LPS configuration lacks the authority to significantly impact HPC SM during acceleration transients.

B. Monte Carlo Simulations

Burst and chop transients, similar to those in the previous sub-section, were simulated at 1000 random altitude and Mach number combinations within the flight envelope. The location of these points within the flight envelope are shown in Figure 15. Figure 16 shows the impact on the minimum HPC SM during the acceleration transient while Figure 17 shows the impact on minimum LPC SM during the deceleration transient. The LPS configuration has the authority to positively impact LPC SM but lacks the authority to significantly and consistently improve HPC SM. The combination of the LPS configuration with the new simplified acceleration schedule actually reduces the minimum HPC SM during transients, at some flight conditions. The dual spool configuration and HPS configuration appear to provide the authority necessary to positively impact the operability of both shafts. Improvements in the minimum HPC SM range from 2.5% to 5.6%. Improvements in the LPC SM are similar for all configurations and are observed to be as much as 3.7% above the baseline. At high Mach numbers and low altitude, the LPC SM benefit appears to dwindle. The reason is because the natural response of the LPC SM tends not to undershoot at these operating conditions. Thus, the best that can be done is to match the baseline results.

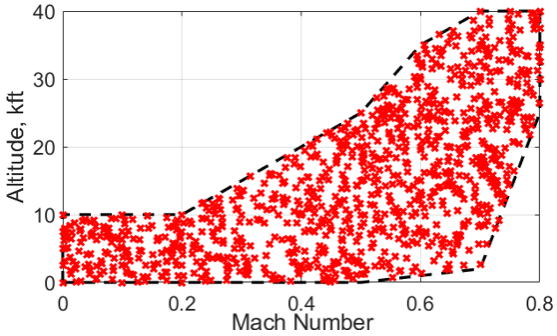

Figure 15.—AGTF30 flight envelope with Monte Carlo test points indicated by the red "x's".

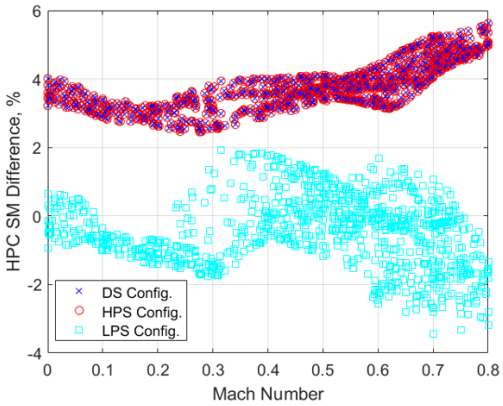

Figure 16.—Minimum HPC SM improvement over the baseline engine model during an acceleration transient.

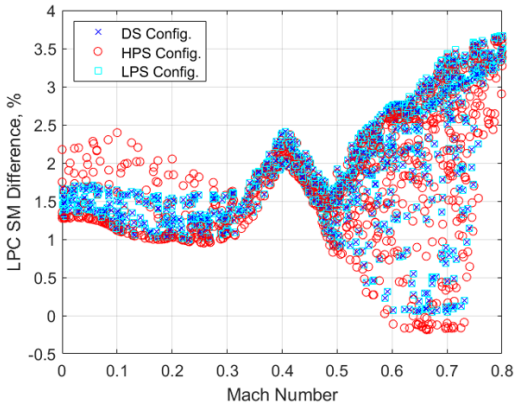

Figure 17.—Minimum LPC SM improvement over the baseline engine model during a deceleration transient.

C. Full Flight

Each TEEM configuration was implemented in simulation with a commercial transport flight mission. The flight profile was constructed from real flight data provided by Reference 21. The flight had a duration of approximately an hour and a half. The profile has the typical flight segments of a commercial flight including a take-off, climb, cruise, descent, and landing. There are numerous changes in throttle setting as the pilot maneuvers the aircraft. The parameters that define the flight profile are plotted in Figure 18. The parameter dT is the difference between the actual ambient temperature and the standard day ambient temperature. The most extreme transient occurs during the first increase in power. Figure 19(a) and (b) plot the HPC SM and LPC SM during this transient. As one can see, the dual-spool and HPS configurations show substantial improvements to the HPC SM while only a modest improvement in HPC SM is observed for the LPS configuration. Figure 19(b) does show an undesirable reduction in LPC SM for the LPS configuration during the transient. Recall that a similar finding was observed for the simulated acceleration results presented in Figure 10(b). For the same transient there is also an observable reduction in the peak HPC discharge pressure (p3) and turbine inlet temperature (T4) as can be seen in Figure 20(a) and (b), respectively. Another metric of interest is the total amount of energy consumption. The super-capacitor supplies power during acceleration transients. It also provides power during deceleration transients for the HPS configuration. The bar graph in Figure 21 shows the energy supplied by the super-capacitors through the entire flight. The amount of energy supplied by the super-capacitors during the entire flight was 0.34 to 1.7 kW-hr, which is on the order of the amount of energy that is present in a typical car battery. The HPS configuration required the most energy due to its use of power input during decelerations. During the course of the flight, the resistor bank in the LPS configuration dissipated ~4 kW-hr of energy. Shown in Figure 22 is a plot of the super-capacitors state of charge, which illustrates the charge and discharge cycles. It can be observed that the EMs are only being used during a very small fraction of the flight's duration. It is also evident that the super-capacitors do not discharge much, which implies that the power supply system may be over-sized.

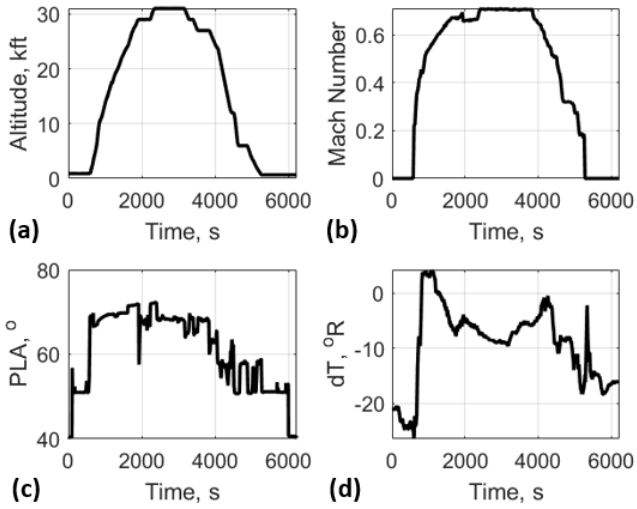

Figure 18.—Full flight, flight profile defined by altitude (a), Mach number (b), power lever angle (c), and the difference between the ambient temperature and the standard atmosphere ambient temperature (d).

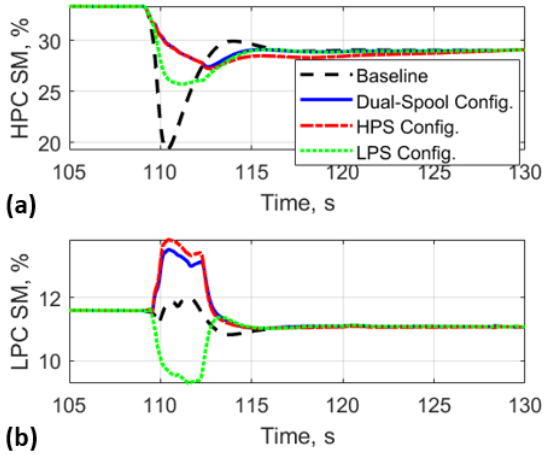

Figure 19.—HPC SM (a) and LPC SM (b) during the first acceleration.

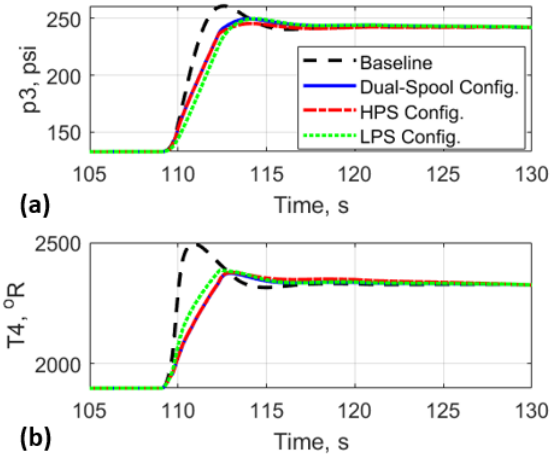

Figure 20.—P3 (a) and T4 (b) during the first acceleration.

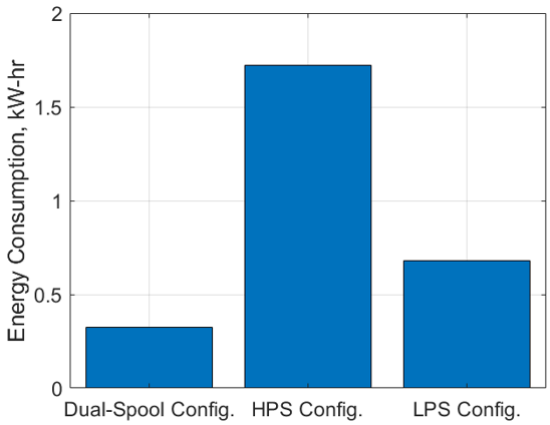

Figure 21.—Energy expended by the super-capacitor bank.

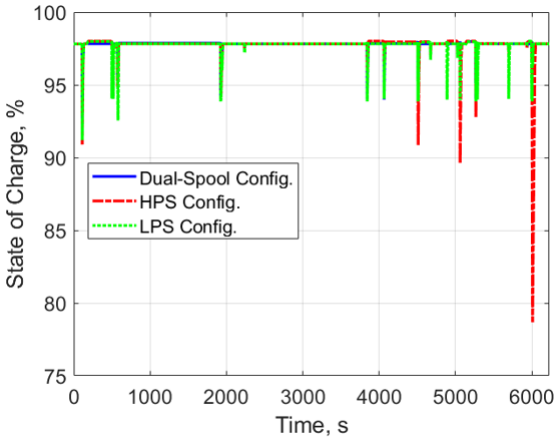

Figure 22.—Super-capacitor state of charge.

VII. Conclusions

A control approach has been demonstrated that applies components of the Turbine Electrified Energy Management (TEEM) concept to an advanced geared turbofan with two spools. The control approach improves transient operability while preserving steady-state performance and utilizing simplified acceleration and deceleration limit logic. Since TEEM utilizes energy storage to provide power to the engine during transients, the control logic has incorporated a charging strategy to reduce the amount of energy storage required. To accommodate charging, the controller applied modified variable bleed valve (VBV) and variable area fan nozzle (VAFN) schedules. Simulation results demonstrated the successful coordination of operability goals and robustness to fuel flow bias. Three different configurations were considered including the use of electric machines (EMs) on both shafts and a single EM on either spool. The control approach has demonstrated operability benefits throughout the flight envelope. This modeling and simulation investigation promotes the feasibility of the TEEM technology. Results suggest that the use of a single EM on the low pressure spool is inadequate to substantially impact operability on the high pressure spool. Furthermore, the potential need to dissipate large amounts of power could make it impractical. However, a single EM on the high pressure spool did exhibit the ability to positively and substantially impact the operability of both spools. While this option may require more energy storage, it will not include a low pressure spool (LPS) EM or any of its supporting electrical equipment. The dual-spool configuration also provided similar operability benefits while eliminating the need for a bleed resistor bank that is present in the LPS configuration. It may also reduce the amount of energy storage that is required compared to the HPS configuration. Minimum high pressure compressor (HPC) and low pressure compressor (LPC) stall margin (SM) benefits were observed to be as much as 5.6% and 3.7%, respectively. For a full flight simulation scenario with a flight profile constructed from real flight data, the TEEM controller was observed to increase the minimum HPC SM by 7% during the flights most aggressive transient and the total amount of energy supplied by onboard energy storage was similar to the amount of energy present in a common car battery. In the future, it is desired to evaluate the net benefit of applying the TEEM concept through re-designing the turbomachinery to take advantage of the ability to more tightly control the operability of the engine.

References

1. Friedrich, C., and Robertson, P.A., “Hybrid-Electric Propulsion for Aircraft,” Journal of Aircraft, Vol. 52, No. 1 (2015), pp. 176–189.
2. Jansen, J.H., Bowman, C., Jankovsky, A., Dyson, R., and Felder, J., “Overview of NASA Electrified Aircraft Propulsion Research for Large Subsonic Transports,” AIAA Propulsion & Energy Forum, Atlanta, GA. 2017.
3. Bowman, C., Felder, J., and Marien, T., “Turbo- and Hybrid-Electric Aircraft Propulsion Concepts for Commercial Transport,” AIAA Propulsion and Energy Forum, Cincinnati, OH. 2018.
4. Hyun, D., Perry, A.T., and Ansell, P.J., “A Review of Distributed Electric Propulsion Concepts for Air Vehicle Technology,” AIAA Propulsion and Energy Forum, Cincinnati, OH. 2018.
5. Johnson, W., Silva, C., and Solis, E., “Concept Vehicles for VTOL Air Taxi Operations,” Report Number ARC-E-DAA-TN50731. 2018.
6. Welstead, J.R., Felder, J., “Conceptual Design of a Single-Aisle Turboelectric Commercial Transport with Fuselage Boundary Layer Ingestion,” AIAA SciTech Forum, San Diego, CA. 2016.
7. Antcliff, K.R., and Capristan, F.M., “Conceptual Design of the Parallel Electric-Gas Architecture with Synergistic Utilization Scheme (PEGASUS) Concept,” 18th AIAA/ISSMO Multidisciplinary Analysis and Optimization Conference, AIAA AVIATION Forum, Denver, CO. 2017.
8. Culley, D., Kratz, J., and Thomas, G., “Turbine Electrified Energy Management (TEEM) For Enabling More Efficient Engine Designs,” AIAA Propulsion & Energy Forum, Cincinnati, OH. 2018.
9. Chapman, J., and Litt, J., “Control Design for and Advanced Geared Turbofan Engine,” AIAA Propulsion & Energy Forum, Atlanta, GA, 2017.
10. Antcliff, K.R., Guynn, M.D., Marien, T.V., Wells, D.P., Schneider, S.J., and Tong, M.T., “Mission Analysis and Aircraft Sizing of Hybrid-Electric Regional Aircraft,” AIAA-2016-1028, AIAA SciTech, 54th AIAA Aerospace Sciences Meeting, San Diego, CA, January 4–8, 2016.
11. Thomas, G., Culley, D., Kratz, J., and Fisher, K., “Dynamic Analysis of the hFan, a Parallel Hybrid Electric Turbofan Engine,” AIAA Propulsion & Energy Forum, Cincinnati, OH, 2018.
12. Chapman, J., Lavelle, T., May, R., Litt, J., and Guo, T.-H., “Toolbox for the Modeling and Analysis of Thermodynamic Systems (T-MATS) User’s Guide,” NASA/TM—2014-216638, 2014.
13. Jones, S., Haller, W., and Tong, M., “An N+3 Technology Level Reference Propulsion System,” NASA/TM—2017-219501, 2017.

14. May, R.D., Csank, J., Lavelle, T.M., Litt, J. S., and Guo, T.-H., "A High-Fidelity Simulation of a Generic Commercial Aircraft Engine and Controller," Proceedings of the 46th AIAA/ASME/SAE/ASEE Joint Propulsion Conference, AIAA-2010-6630, Nashville, TN, July 2010.
15. Chapman, J., and Litt, J., "An Approach for Utilizing Power Flow Modeling for Simulations of Hybrid Electric Propulsion Systems," 2018 AIAA/IEEE Electric Aircraft Technologies Symposium, Cincinnati, OH, July 2018.
16. Bradley, M.K., and Droney, C.K., "Subsonic Ultra Green Aircraft Research: Phase II -Volume II – Hybrid Electric Design Exploration," NASA/CR—2015-218704/Volume II. April, 2015.
17. Kratz, J., Culley, D., and Thomas, G., "Evaluation of Electrical System Requirements for Implementing Turbine Electrified Energy Management," AIAA Propulsion & Energy Forum, Indianapolis, IN, 2019.
18. Simon, D., Garg, S., "Optimal Tuner Selection for Kalman Filter Based Aircraft Engine Performance Estimation," GT2009-59684, ASME Turbo Expo Conference, Jun. 8–12, 2009, Orlando, FL.
19. Kratz, J., and Thomas, G., "Dynamic Analysis of the STARC-ABL Propulsion System," AIAA Propulsion & Energy Forum, Indianapolis, IN, 2019.
20. Federal Aviation Administration, "Title 14 of the Code of Federal Regulations," https://www.ecfr.gov/cgi-bin/text-idx?SID=2df09c833c6cae09d18ba3a5ae91abb0&mc=true&node=se14.1.33_173&rgn=div8, accessed January, 2019.
21. "Sample Flight Data." DASHlink -. Web. 17 April 2019. https://c3.nasa.gov/dashlink/projects/85/resources/